Earth Surface Processes and Landforms
Earth Surf. Process. Landforms **24**, 1095–1114 (1999)

PORE WATER PRESSURE AND STREAMBANK STABILITY: RESULTS FROM A MONITORING SITE ON THE SIEVE RIVER, ITALY

NICOLA CASAGLI*, MASSIMO RINALDI, ALESSANDRO GARGINI AND ANDREA CURINI
[1]*Department of Earth Science, University of Florence, Via G. La Pira 4, 50121 Florence, Italy*

Received 30 November 1997; Revised 16 December 1998; Accepted 18 February 1999

ABSTRACT

To investigate the role of pore water pressures in the stability of a streambank, a series of tensiometers and piezometers was installed in a bank of the Sieve River, Tuscany, Italy. Fluvial entrainment at the bank toe was monitored by repeated cross-profiling, erosion pins and marked pebbles. Fluctuations in matric suction measured at the tensiometers reflected the overall response of pore water pressures to rainfall, evapotranspiration, rising and drawdown of the river stage, and variations in water table. An expression was derived for the safety factor with respect to mass movement of the upper bank, incorporating the failure criterion for unsaturated soils and the normal Mohr–Coulomb criterion for saturated conditions. Variations in matric suction have important effects on the stability of the streambank. During low-flow periods, the shear strength term due to the matric suction allows the bank to remain stable at a steep angle. However, during rainfall and flow events, reduction in matric suction and increase in unit weight of the material from vertical and lateral infiltration may be sufficient to trigger a mass failure, without development of significant positive pore water pressures. During the rising limb of high-flow events, the factor of safety increases as a consequence of the stabilizing confining pressure of the water in the river, despite a reduction in matric suction. During drawdown in the river, when the suction values are still low and the confining pressure in the river decreases to zero, the factor of safety falls to lower values than those experienced prior to the runoff event. Measurements of fluvial entrainment reveal that, although the processes, mechanisms and the frequency of retreat of basal and upper bank zones differ significantly, the amount of retreat at the bank toe due to fluvial erosion is comparable to that of the upper portion of the bank due to mass failure. Copyright © 1999 John Wiley & Sons, Ltd.

KEY WORDS: pore water pressure; matric suction; streambank stability; Sieve River, Italy

INTRODUCTION

Bank erosion processes represent an important factor in driving planform changes, meander development and channel width adjustments in alluvial rivers. Streambank erosion may also be a significant river management problem because it may be responsible for land loss, damage to structures adjacent to the river channel, delivery of excessive volumes of sediment to downstream reaches, and alterations to the relationship between river stage and the phreatic surface beneath the floodplain.

Bank retreat results from a complex combination of processes of fluvial erosion and mechanisms of mass failure (Hooke, 1979; Thorne and Tovey, 1981; Thorne, 1982; Lawler *et al.*, 1997). Many aspects of streambank erosion and instability are still not well understood because of difficulties associated with monitoring the parameters involved. Notwithstanding the development of recent automatic technologies capable of monitoring the timing and rates of bank retreat in detail (Lawler, 1991), few data are available to identify the causes of erosion or instability. A particular area of uncertainty concerns temporal changes in pore water pressures within the bank, as these are fundamental in determining its stability with respect to mass failure (Wolman, 1959 ; Twidale, 1964; Hooke, 1979; Thorne, 1982).

Understanding the role of pore water pressures in determining bank instability is therefore necessary to improve existing methods of riverbank stability analysis and models of channel evolution. Stability analyses commonly applied to riverbanks (Lohnes and Handy, 1968; Selby, 1982; Huang, 1983; Simon *et al.*, 1991;

* Correspondence to: N. Casagli, Department of Earth Science, University of Florence, Via G. La Pira 4, 50121 Florence, Italy
Contract/grant sponsor: Italian National Research Council Group for Hydro-geological Disaster Prevention

CCC 0197-9337/99/121095–20 $17.50

Osman and Thorne, 1988; Darby and Thorne, 1996) typically use concepts from classical saturated soil mechanics, neglecting the stabilizing effects of negative pore pressures in the unsaturated portion of the bank. In fact, streambank material is normally in a condition of partial saturation, and is therefore subject to negative pore water pressures (suctions) that produce an increase in apparent strength.

To investigate quantitatively the impact of negative pore pressures on bank stability, a monitoring programme was initiated during February 1996 on a streambank of the Sieve River, Tuscany, Italy. The objectives of this on-going programme are: to achieve a better understanding of the factors and mechanisms determining bank stability and failure; to improve methods of bank stability analysis by incorporating the effects of negative pore water pressure or suction; and to investigate interactions between fluvial erosion processes and mechanisms of mass failure in controlling bank morphology and the long-term retreat rate.

The site was instrumented using an array of tensiometers and piezometers. The banks of the Sieve River are well suited for this type of monitoring as they are composed of sand and silt deposited by overbank flows, underlain by a basal layer of gravel. The sandy silt portions of the banks remain substantially stable at steep angles until major flow events occur. Preliminary results and interpretations for the first six months of monitoring have previously been reported by Casagli *et al.* (1996, 1997). Spatial variability in stability of the Sieve River streambanks, taking into consideration the effects of negative pore water pressures and applying concepts and methods of unsaturated soil mechanics, is discussed by Rinaldi and Casagli (1999). In that paper, changes in the stability of an individual streambank through time are also investigated using some of the monitoring results. In this paper, a more complete description of temporal variations in pore water pressures and water movements within the bank is presented, based on the results of 16 months of monitoring. Direct measurements of the matric suction have provided the opportunity to apply a rigorous bank stability analysis and thereby obtain the trend of factor of safety through time. A bank failure during the monitoring period, on 14 December 1996, has enabled us to validate the stability analysis.

The paper makes use of the monitoring and modelling results to determine the variability of pore water pressures in a streambank at a seasonal scale and evaluate their response to rainfall and single flow events; to evaluate the contribution of matric suction to increase shear strength in partly saturated material and assess the role of suction in determining bank stability; to determine the influence of reduction in matric suction during flow events in causing instability and triggering mass failures; and to illustrate differences in the frequency of occurrence of fluvial erosion (acting on the basal portion of the bank) and mass failures (occurring on the upper part of the bank).

THEORETICAL CONSIDERATIONS OF UNSATURATED SOIL MECHANICS AND THEIR APPLICATION TO STREAMBANK STABILITY ANALYSIS

In this section some of the fundamental theoretical aspects of unsaturated soil mechanics are briefly reviewed to provide the theoretical basis for the following sections. Possible applications of these concepts in analysing the stability of streambanks are discussed.

Pore water pressure and effective stress

The fundamental influence of pore water pressure on the mechanical properties of soils was first recognised by Terzaghi (1923), who developed the principle of effective stress. Pore water pressure is defined as the pressure of water filling the voids between solid particles. In fully saturated soils all the voids are filled by water and, under these conditions, the effective stress (σ') is given by the difference between the total normal stress (σ) and the pore water pressure (u_w).

In the case of partially saturated soils the voids are occupied partly by water and partly by air. The pore water pressure (u_w) must always be less than the pore air pressure (u_a) due to surface tension at the air–water interface. As u_a is assumed to be in equilibrium with atmospheric pressure (i.e. zero gauge pressure), pore water pressure (u_w) in the unsaturated portion above the water table is negative. The difference between the two quantities ($u_a - u_w$) is defined as *matric suction* and is a positive quantity because $u_w < 0$. Measurements of matric suction can be made *in situ* using tensiometers (Fredlund and Rahardjo, 1993).

Shear strength criterion for unsaturated soils

The presence of matric suction in an unsaturated soil increases the shear strength of the material. For an unsaturated soil the failure criterion can be expressed in term of two stress state variables: the net normal stress $(\sigma - u_a)$, and the matric suction $(u_a - u_w)$, as in the following form proposed by Fredlund *et al.* (1978):

$$\tau = c' + (\sigma - u_a)\tan\phi' + (u_a - u_w)\tan\phi^b \tag{1}$$

where τ = shear strength, c' = effective cohesion, ϕ' = friction angle in terms of effective stress and ϕ^b = angle expressing the rate of increase in strength relative to the matric suction. The angle ϕ^b is always lower than ϕ' and values typically range between 7° and 26° (Fredlund and Rahardjo, 1993).

This criterion represents an extension of the traditional Mohr–Coulomb failure envelope in terms of effective stress because as the soil approaches full saturation the pore water pressure u_w tends to be equal to u_a and the suction component disappears. The extended Mohr–Coulomb failure envelope for an unsaturated soil can be plotted in a three-dimensional diagram with the shear stress, τ, and the two stress state variables, $(\sigma - u_a)$ and $(u_a - u_w)$, on the three axes (Fredlund and Rahardjo, 1993). The extended failure envelope can be presented as a projection onto the shear stress versus $(\sigma - u_a)$ plane. For a given matric suction value, the projection is a line given by the equation:

$$\tau = c_a + (\sigma - u_a)\tan\phi' \tag{2}$$

where c_a = total cohesion (or apparent cohesion) intercept, which incorporates the effects of the matric suction and of the effective cohesion:

$$c_a = c' + (u_a - u_w)\tan\phi^b \tag{3}$$

Unsaturated flow

The pore water pressure distribution within a soil also controls the seepage both in the saturated and in the unsaturated zone. The flow of water in saturated and unsaturated, porous media such as soil is generally described by Darcy's law (Richards, 1931; Fredlund and Rahardjo, 1993). In unsaturated flow the permeability is a function of the degree of saturation, and the effects of matric suction have to be included in the expression of the hydraulic head, by considering the negative pressure head (matric head) h_m:

$$h_m = -\frac{(u_a - u_w)}{\gamma_w} \tag{4}$$

where $(u_a - u_w)$ = matric suction and γ_w = unit weight of water.

The total head h is obtained by the algebraic sum of the evaluation head z and the matric head h_m:

$$h = z - \frac{(u_a - u_w)}{\gamma_w} \tag{5}$$

The flow of water always occurs from points with higher total head towards points with lower total head. The hydraulic gradient both in the saturated and in the unsaturated zone is obtained by dividing the total head by the distance between the two points measured along the flow path.

Applications to streambanks

In the unsaturated portion of a riverbank both the shear strength of the material and the conditions of seepage are strictly controlled by the distribution of matric suction. The apparent cohesion due to matric suction can represent a substantial component of the total shear strength. As a result, in banks like those of the

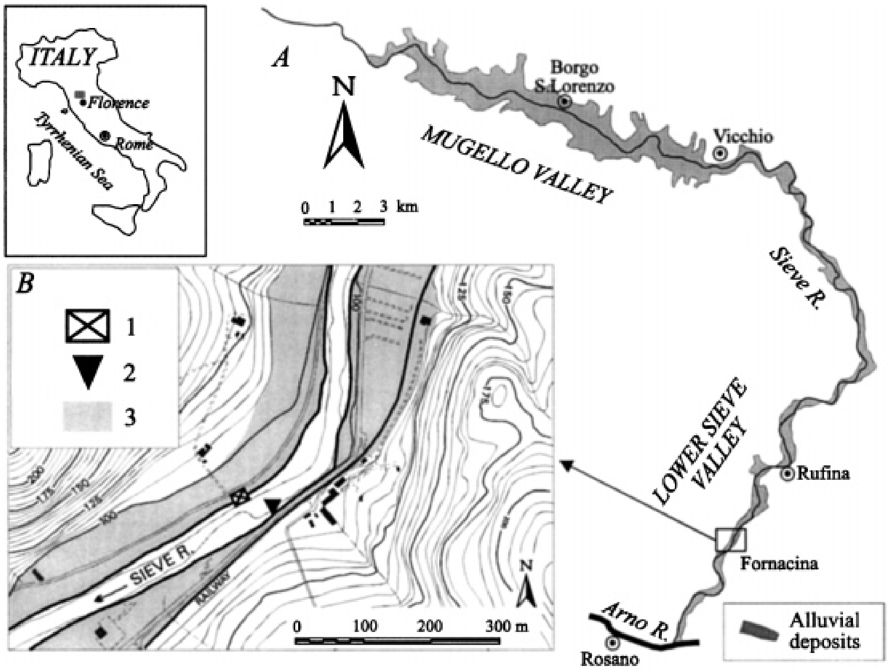

Figure 1. Location map for the Sieve River, central Italy. (A) Sieve River course. (B) Location of the study site. Key: 1, monitored bank; 2, gauging station; 3, alluvial deposits

Sieve River, which are composed of granular soil (that is, with fine sand as a dominant component), the shear strength term due to the matric suction allows banks to remain stable during low-flow periods at angles much steeper than the effective friction angle (Rinaldi and Casagli, 1999). Negative pore water pressures in streambanks fluctuate frequently due to rainfall, variations of river stage, evapotranspiration, and variations of the capillary fringe sustained by the water table. During rainfall and rising stages, changes in bank storage (Sharp, 1977) cause an increase in water content and in pore water pressure due to the rising water table. During a major flow event the bank material can become fully saturated, so that the apparent cohesion disappears and positive pore water pressures occur. Under these conditions stability can still be maintained due to the confining pressure of the water in the river channel on the bank face.

However, bank failures are likely to occur during drawdown following a high stage, when the bank material is still at or near saturation and the confining pressure of the river is removed (Twidale, 1964; Thorne, 1982; Springer *et al.*, 1985 ; Lawler *et al.*, 1997). Drawdown induces a process of transient seepage during which the water table lowers progressively until a new equilibrium with the boundary conditions is reached, and the pre-event suction levels are re-established.

STUDY AREA

The Sieve River is a tributary of the Arno River, the largest stream of Tuscany, Italy. The area of the Sieve catchment at the confluence with the Arno is about 840 km^2, and the total length of the river is 58 km. In the upper half of its course, the river flows along a wide alluvial valley cut into fluviolacustrine deposits of the Mugello intermontane basin, where it displays the features typical of alluvial channels. In its lower course the Sieve flows in a narrow valley, where the channel is partially confined and its configuration is often controlled by bedrock (Figure 1).

The morphological evolution of the channel and its alluvial plain during the last few centuries have been influenced by human disturbances linked to land-use changes in the catchment. In previous centuries, intense deforestation caused considerable aggradation of the alluvial plain (Rinaldi and Rodolfi, 1995). Subsequent

Table I. Main morphological, sedimentological and hydrological data of the study site at Fornacina

Catchment area, A	831 km^2
Channel width, W	64 m
Channel gradient, S	0·003
Bed bottom elevation, z_o	92 m a.s.l.
Bed material grain size, D_{50}	62 mm
Bar material grain size, D_{50}	5 mm
Bank toe grain size, D_{50}	14 mm
Upper bank grain size, D_{50}	0·09 mm
Minimum mean daily discharge, q_{min}	0·31 m^3 s^{-1}
Average of mean daily discharge, q_{50}	15·7 m^3 s^{-1}
Maximum mean daily discharge, q_{max}	917 m^3 s^{-1}
Mean of annual peak discharges, Q_m	448 m^3 s^{-1}
Maximum of annual peak discharges, Q_{max}	1340 m^3 s^{-1}

in-stream gravel mining and reduced sediment supply due to reforestation and upland sediment retention have caused rapid channel-bed lowering during recent decades, leading to bank instability (Rinaldi, 1995; Rinaldi and Casagli, 1999).

The annual rainfall distribution displays a minimum in July, and two maxima: one in November and the other at the end of the winter. The climate can be classified as *Csa* type, according to the Köppen (1936) classification. That is, temperate with a dry summer and temperatures higher than 22°C during the warmest month. Annual rainfall (period 1921–1980) ranges from 1000 to 1400 mm.

The study site is located at a gauging station (Fornacina) of the National Hydrological Survey, along an alluvial reach in the lower part of the Sieve valley (Figure 1). Morphological, sedimentological and hydrological data describing the study site are summarized in Table I. Channel width, gradient and bed elevation were obtained by detailed topographic surveys. Bed, bank toe and upper bank material grain sizes were measured by volumetric sampling followed by standard sieve analyses, while grid sampling was adopted to determine the bar grain size. Minimum, average, maximum daily and annual peak discharges were obtained from data at the Fornacina gauging station for the period of record 1931–1993.

The monitoring site was selected on the basis of three criteria. First, the streambank was actively retreating through a combination of fluvial erosion and mass failures, but the rate of retreat was not so high that it created excessive risk of damage to the monitoring station. Second, the site was sufficiently close to a gauging station that it was possible to use stage readings at the gauging station to establish the time series, frequencies and water surface elevations of discharges at the bank site. Third, the morphology, sedimentology and dominant erosion processes of the study bank were representative of streambanks along the Sieve and other rivers in central Italy.

The monitored streambank is composite, using the terminology of Thorne and Tovey (1981), with a basal layer of sandy gravel, 1·7 m thick, and an upper layer of sandy silt, 2·5 m thick. The basal layer can be divided into two units with different friction angles and resistance to fluvial entrainment. The higher unit is composed of *in situ* gravel closely packed and imbricated with interstitial sand and a bank slope of about 70°. The lower unit is mainly composed of loose gravel that has accumulated at the toe of the bank due to the combined effects of fluvial erosion and weathering, and has a bank slope of about 25°.

SOIL CHARACTERISTICS

The geotechnical stratigraphy of the bank (Figure 2) was obtained by combining field observations with analyses of cores extracted from hand-drilled boreholes, and the results of one static (CPT) and two dynamic penetration tests (SCPT). Laboratory tests were performed to characterize the material of the upper layer, which is subject to mass failures. The soil can be classified as a silty fine sand (gravel fraction $GF = 5$ per cent, sand fraction $SF = 68$ per cent, silt fraction $MF = 21$ per cent, clay fraction $CF = 6$ per cent) according to the Unified Soil Classification System (Wagner, 1957), with a coefficient of uniformity $U = D_{60}/D_{10} = 36$ and

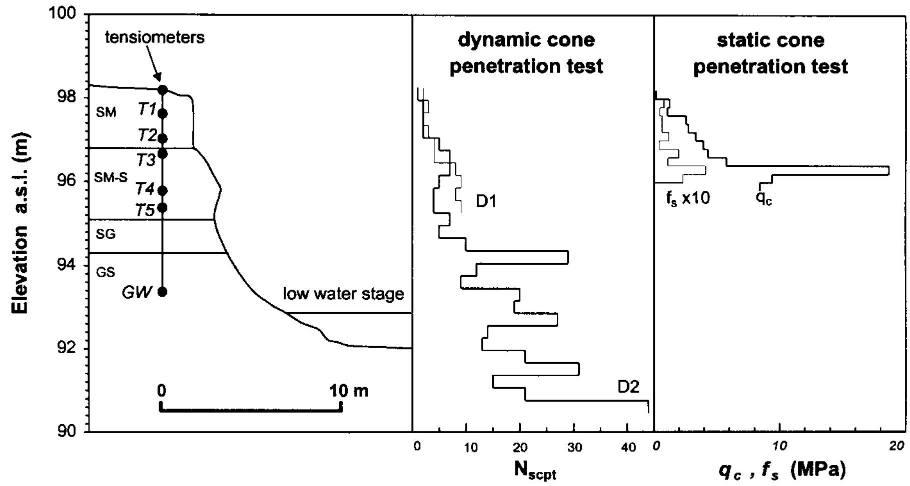

Figure 2. Geotechnical profile of the bank and results of penetration tests. SM, sandy silts and silty sands; SM–S, sands and silty sands; SG, sands with gravel; GS, packed sandy gravels. T1, T2, T3, T4, piezo-tensiometers; D1, D2, dynamic cone penetration tests; N_{scpt} = standard cone penetration number. Static cone penetration test: q_c = cone resistance; f_s = skin friction

a porosity n = 42–44 per cent. The unit weight (γ) varies between 16·5 and 19·3 kN m^{-3}, depending on the degree of saturation. The saturated permeability of the upper layer was assessed from *in situ* seepage tests, which yielded an average value of $6{\cdot}0 \times 10^{-6}$ m s^{-1} (Curini, 1998).

The shear strength of the upper layer was evaluated using borehole shear tests (BST) (Lutenegger and Halberg, 1981), carried out about 1 m below the ground surface, where the soil was subject to negative pore water pressures. For this reason the test was interpreted in terms of the Fredlund *et al.* (1978) criterion, incorporating the effect of matric suction into the apparent cohesion term (Rinaldi and Casagli, 1999). The test, interpreted in this way, provided a linear relationship between the net normal stress ($\sigma - u_a$) and the shear strength, in a stress interval ranging between 0 and 40 kPa. The results indicated shear strength parameters of $\phi = 38°$ and $c_a = 2$ kPa.

Laboratory triaxial tests on saturated samples, performed in the stress range 25 to 75 kPa, allowed the measurement of a friction angle in terms of effective stress. The results indicated that the effective friction angle (ϕ') was 33°, while the effective cohesion (c') was zero. Taking into account the grain size of the soil, the triaxial test value of ϕ' appears more reliable than that obtained from the BST. Overestimation of ϕ' using the BST probably results from underestimation of the apparent cohesion. Back analysis of the BST results, coupled with tensiometric measurements, produced a mean estimation for the angle ϕ^b of 16°, but there was wide scatter in the data with values ranging from 10° to 26°.

A series of measurements of water content was made for a wide range of matric suctions in the upper layer and the soil water characteristic curve was determined by applying the method of Brooks and Corey (1964). A relationship linking the bulk unit weight to matric suction was then derived from the soil water characteristic curve, using:

$$\gamma = \gamma_w(G_s + Se)/(1 + e) \tag{6}$$

where γ_w = unit weight of the water, G_s = specific gravity, S = degree of saturation and e = void ratio, linked to the soil total porosity (n) by the expression: $e = n / (1 - n)$.

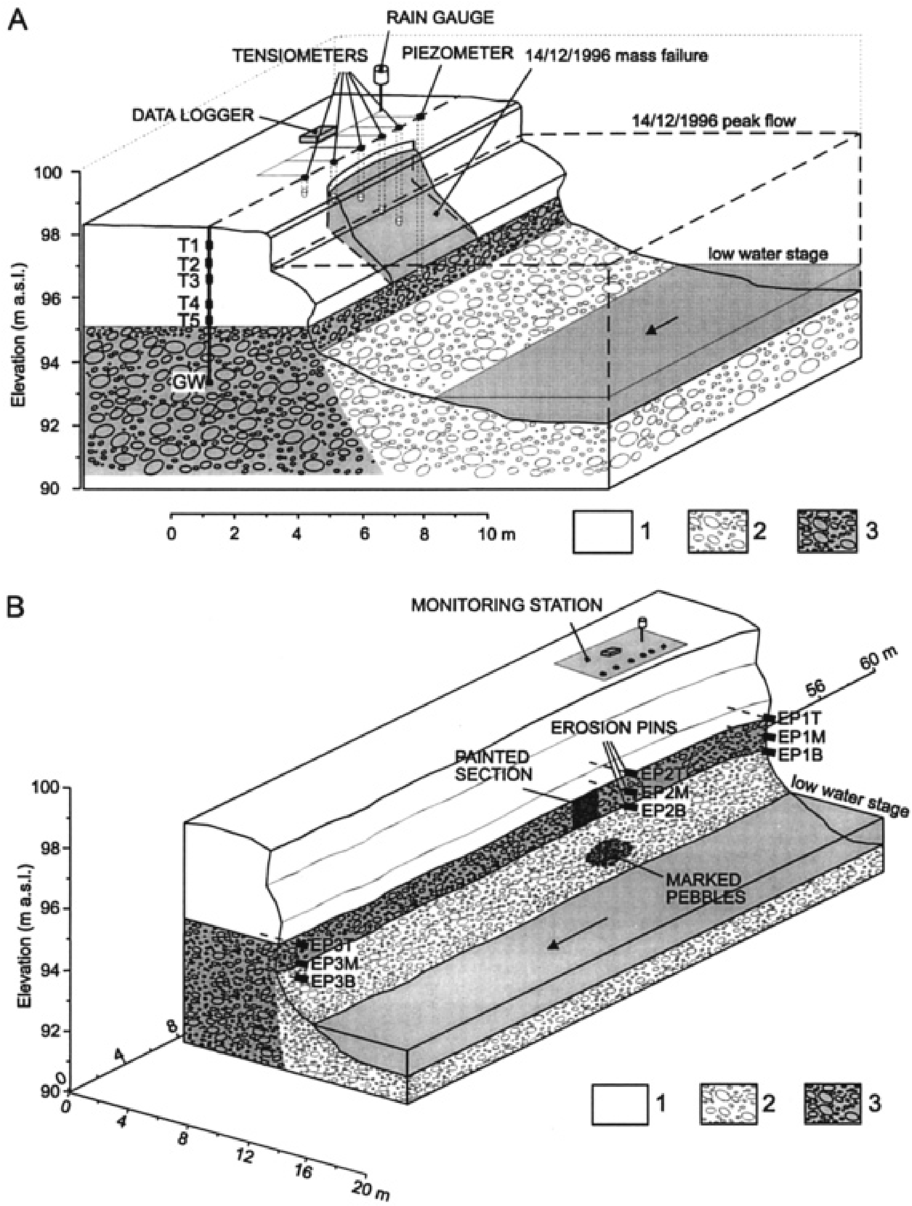

Figure 3. Sketch of the monitored reach. (A) Monitoring station. (B) River reach covered by fluvial entrainment study. Key: 1, Silt and sand; 2, loose gravel; 3, packed gravel with interstitial sand

MONITORING INSTRUMENTATION

Pore pressure, rainfall and river stage measurements

Instrumentation installed at the experimental site consists of pressure transducer tensiometers, a pressure transducer piezometer and a rain gauge (Table II; Figure 3A), all connected to a data logger that records the data every 30 min.

Table II. Details of monitoring instrumentation

Label	Instrument	Measured parameter	Unit	Accuracy	Depth (m)	Elevation (m a.s.l.)	Date of installation
T1	Tensiometer	Matric suction	hPa	±1 hPa	0·6	97·6	5/02/96
T2	Tensiometer	Matric suction	hPa	±1 hPa	1·1	97·1	5/02/96
T3	Tensiometer	Matric suction	hPa	±1 hPa	1·5	96·7	5/02/96
T4	Tensiometer	Matric suction	hPa	±1 hPa	2·4	95·8	5/02/96
T5	Tensiometer	Matric suction	hPa	±1 hPa	2·8	95·4	18/01/97
GW	Piezometer	Positive pressure head	cm	±1 cm	4·8	93·4	18/01/97
R	Rain gauge	Rainfall	mm	±1 mm	-	-	18/10/96

The negative pore water pressure measured by tensiometers is numerically equal to the matric suction ($u_a - u_w$) when the pore air pressure is atmospheric ($u_a = 0$). The tensiometers provide direct measurements of matric suction in the range −1000 hPa to 850 hPa, with an accuracy of ±1 hPa. Above the value of 850 hPa tensiometers are subject to cavitation when, due to the high suction, air bubbles form in the porous cup, hindering accurate measurements at the transducer. The value of 850 hPa therefore represents an upper limit to suction measurement using tensiometers. When the soil becomes fully saturated, the apparatus works as a piezometer as it is also able to measure negative water tension (that is positive pore water pressure). The transducer permits measurement of positive water pressures up to 1000 hPa.

During the first phase of the monitoring programme (5 January 1996 to 18 October 1996) four tensiometers were installed in the upper layer of the bank, with the porous cups at various depths (Table II). During this period hourly rainfall data were available from a meteorological station of the National Hydrologic Survey located about 5 km southwest at Rosano (Figure 1). To improve the accuracy and detail of rainfall data, on 18 January 1996 a rain gauge was installed at the experimental site. It records rainfall at half-hourly intervals with an accuracy of 0·2 mm.

After about one year of monitoring, it became apparent that data on pore water pressures at greater depths was required. This prompted installation of a piezometer and another tensiometer (T5), on 18 January 1997. The piezometer indicates the instantaneous location of the water table in the bank, with an accuracy of ±1 cm.

During the period of investigation river stages of the Sieve River, recorded every 30 min, were available from the Fornacina gauging station, located 50 m upstream. Simultaneous measurements of river stages at the experimental site and at the gauging station have allowed correlation of data recorded at the gauging station with corresponding stages at the monitored bank.

Fluvial entrainment measurements

Bank retreat in the monitoring reach was measured by repeated cross-profiling from three permanent monuments. Erosion pins, marked pebbles, and a painted portion of the basal bank were used to monitor fluvial entrainment and to support estimation of the critical fluid shear stresses for erosion of materials at the bank toe. The limitations and advantages of these techniques have been discussed in detail by Lawler (1993).

During August 1996 three sets of erosion pins were installed in the basal part of the bank. Each set included three pins inserted horizontally into the bank toe and spaced vertically about 0·5 m (Simon and Darby, 1997). Most pins were installed in the *in situ* matrix of packed gravel with sand or silt (EP1M, EP1B, EP2M, EP2B, EP3T, EP3M), but others were placed in the loose, coarse gravel (EP3B) and silty sand (EP1T, EP2T) (Figure 3B).

A representative portion of the exposed bank surface, composed of packed coarse gravel, fine gravel and sand was painted and 200 pebbles were collected from the loose gravel at the bank toe. These pebbles were painted using four different colours, one for each of the four main size classes (-5ϕ, $-5{\cdot}5\phi$, -6ϕ and $-6{\cdot}5\phi$), and replaced randomly on the top of the loose deposits. An additional set of 77 marked pebbles was prepared and replaced with the same procedure after the flow event of 18 November 1996.

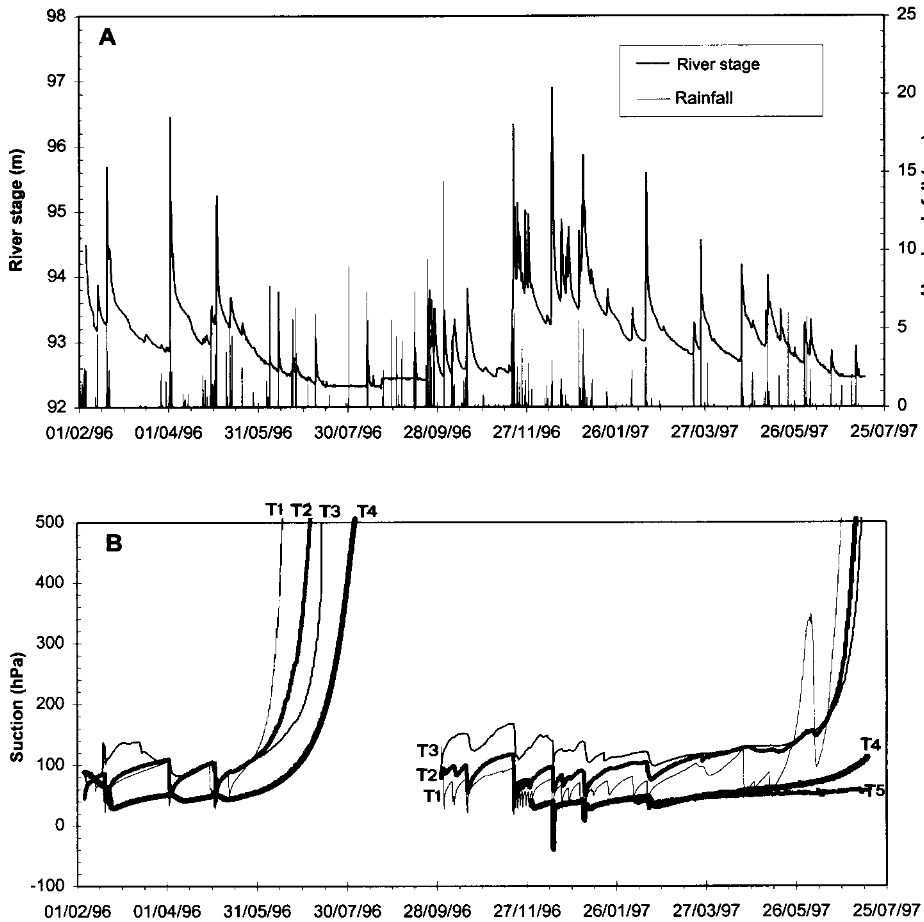

Figure 4. Results of 16-month monitoring programme. (A) Rainfall, river stage and groundwater level. (B) Trend of the matric suction measured at the tensiometers (T1, T2, T3, T4, T5 from the shallowest to the deepest).

MONITORING RESULTS

Seasonal trends in pore water pressure

The results of 16 months of monitoring are illustrated in Figure 4. During the study, rainfall events were, in general, typical of the regional climate, although there were some anomalies. In particular, two dry periods occurred, from 18 October to 18 November 1996 and from 15 February to 20 April 1997, while rainfall was particularly abundant between 18 November and 25 December 1996. During the wet seasons (February to May 1996 and October 1996 to May 1997) matric suction values ranged from 20 to 160 hPa and the suction profile exhibited a maximum near the mid-height of the sandy silt layer (tensiometer T3).

The upper tensiometers (T1 and T2) responded quickly to rainfall through abrupt falls in suction, while the deepest ones (T4 and T5) were only slightly affected by rainfall infiltration, but were influenced by rises in river stage that exceed the elevation of the contact surface between the silty sand layer and the underlying gravel (95·1 m a.s.l.). Pore water pressure changed from negative to positive only once, at T4, in response to the maximum flow observed during the study period, when the river reached an elevation of 97 m a.s.l on 14 December 1996.

At the beginning of the dry season in June 1996, suction values increased progressively and the soil approached a condition of residual saturation in response to the water deficit caused by rainfall deficiency and

strong evapotranspiration. By the end of July 1996, all the tensiometers had reached the instrumental suction limit of 850 hPa. The limit was reached progressively, starting with the uppermost tensiometer (T1) and proceeding downwards. The tensiometers remained out of the instrumental range for the rest of the summer of 1996.

In late September and early October 1996, suction values at T1, T2 and T3 fell within the instrumental range and then fluctuated within the same range observed during the previous summer (20 to 160 hPa). Conversely, T4 suffered cavitation until the end of November 1996. During June and July 1997, the three upper tensiometers (T1, T2 and T3) again progressively reached the instrumental suction limit.

Response to rainfall events

The sensitivity of matric suction to rainfall varied systematically from the shallowest to the deepest tensiometer. For example, Figure 4B indicates that T1 was influenced by an hourly rainfall of 2 mm on 29 April 1996, while T2 (at about twice the depth of T1) was unaffected and required an hourly rainfall of at least 4 mm to register any reduction in suction. Also, matric sensitivity varied seasonally. For example, during June 1996 more than 8 mm of hourly rainfall was needed before a decrease in suction was registered at T1.

The delay time between peak precipitation and peak in total head corresponds to the time necessary for the wetting front to travel from the ground surface to a particular depth in the soil. For a given depth, the delay time tends to increase from humid to dry seasons, due to a reduction in the unsaturated hydraulic conductivity of the soil. For example, at T1 (depth = 0·57 m), delay time varies from 0·1 days in January to 1·8 days in June; while at T4 (depth = 2·41 m), the variation during the same months is from 2·5 to 23 days (Figure 4 B). It is the combined effects of reduced sensitivity to rainfall and increased delay time with depth that explain why the variability in matric suction decreases so markedly with depth.

Response to flow events

Figure 5A presents the hydrograph of the 14 December 1996 flow event, while Figure 5B illustrates the resulting variations in matric suctions. Suction at T1 began to fall prior to the flow peak, in response to wetting by rainfall. Suction decreased from an initial value of about 80 hPa to about 20 hPa, indicating that the infiltrating rainwater did not completely saturate the uppermost portion of the bank. Rainwater infiltration also produced small suction reductions at T2 and T3, which fell from 100 to 60 hPa and 140 to 100 hPa, respectively.

River stage peaked at 97 m a.s.l., exceeding the elevations of tensiometers T3 and T4. However, only T4 seems to have responded directly to lateral seepage and drainage. Suction at T4 fell abruptly from about 40 hPa to a negative value of about −40 hPa before rising to 30 hPa, a value slightly lower than that prior to the event.

Another significant flow event took place on 15 February 1997, when river stage reached a maximum elevation of 95·7 m (Figure 6). During this event the deep piezometer was in operation and it was therefore possible to monitor the relationship between river stage and water table. The water table rise was slightly delayed with respect to the river stage, and the maximum elevation of the water table remained about 1 m lower than the flow peak stage (Figure 6A). This flow event contrasted to that of 14 December 1996, in that it followed a prolonged dry spell that produced low levels of soil saturation. Matric suctions decreased due to rainwater infiltration, with T1 registering the largest drop (Figure 6B). Only T5 was at an elevation below that of the peak stage and it recorded a decrease in matric suction due to capillary rise associated with lateral water transfer from river to bank. However, no positive pore water pressures were generated.

Unsaturated flow

Total head variations over the 16 months of monitoring are shown in Figure 7A. Mean sea level has been taken as datum for the elevation head (z) and the river stage. Variations in hydraulic gradient between adjacent pairs of sensors are shown in Figure 7B. Positive values of hydraulic gradient correspond to downward flow, while negative values indicate upward flow.

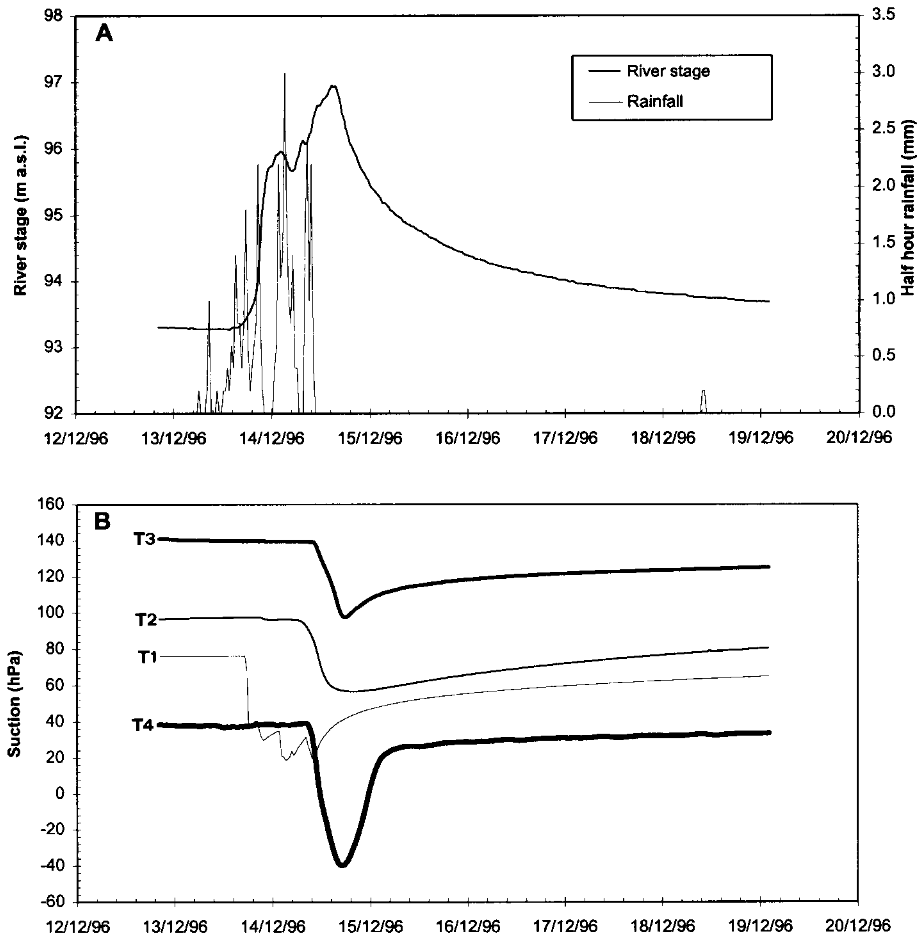

Figure 5. Record of 14 December 1996 flow event. (A) Rainfall and river stages. (B) Variations in suction at the four tensiometers

For most of the monitoring period, and particularly for the winter/spring periods, total head decreases with depth and unsaturated hydraulic gradients are downward. The flow of water in the bank during this period is mainly controlled by rainfall, while evapotranspiration effects are limited. Conversely, vertical water movement is upward during the summer due to the water deficit produced when evapotranspiration exceeds precipitation and the zero flow plane (originally located closed to the ground surface) migrates downward. For example, in 1997 reversal began at the beginning of June in the uppermost portions of the bank and progressively extended to a depth of 3 m by the beginning of July. During particularly low stages in the river, unsaturated water flow directed upwards was observed to extend throughout the bank.

BANK STABILITY

Stability analysis

Seven flow events exceeded a stage of 95·1 m a.s.l. and so reached the upper silty sand layer. However, only during the largest event, on 14 December 1996, did a bank failure occur. The failure occurred some hours after the flow peak. The failure mechanism was planar sliding with a tension crack and the geometry of the

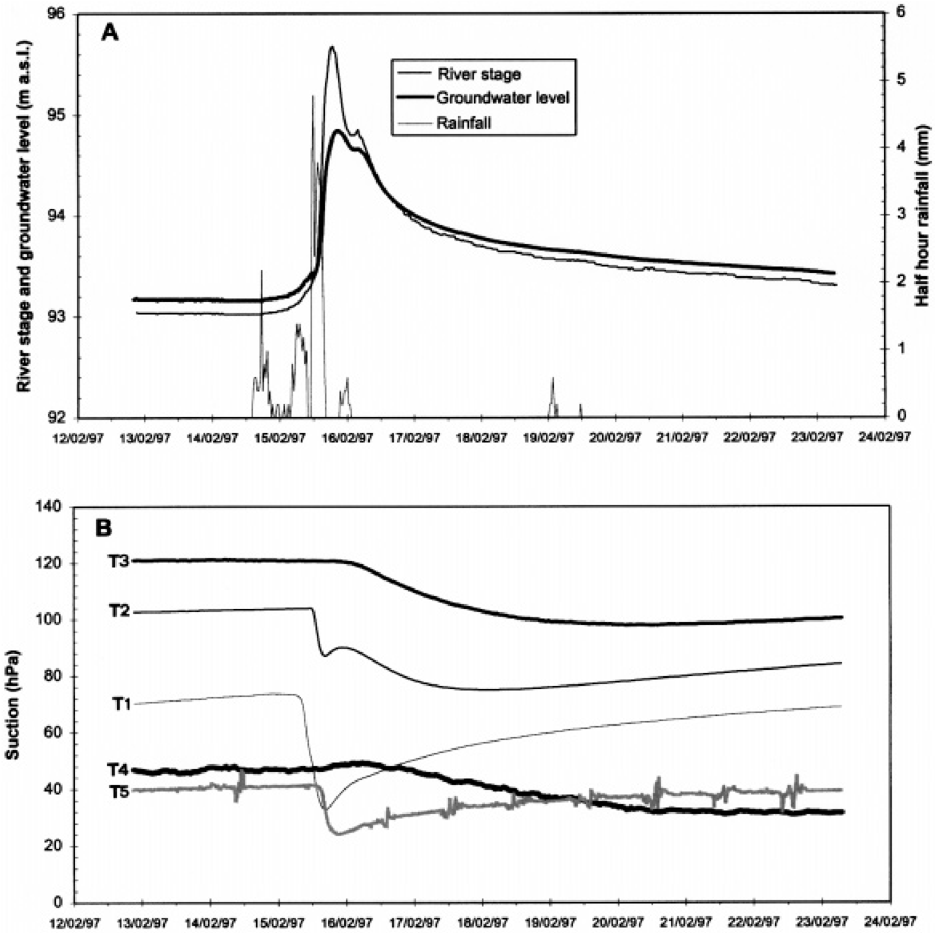

Figure 6. Record of 15 February 1997 flow event. (A) Rainfall, river stage and groundwater level. (B) Variations in suction at the five tensiometers

failure block was reconstructed through repeated profile surveys prior to and immediately following the failure (Figure 8).

Shear strength parameters of the Fredlund *et al.* (1978) criterion for the unsaturated material were $\phi' = 33°$, $\phi^b = 16°$ and $c' = 0$. The mean suction along the failure surface was obtained from a weighted average of the readings at T3, T4 and T5. When a tensiometer recorded a positive pore water pressure, the normal Mohr–Coulomb criterion in terms of effective stress was used to represent the shear strength of failure surface adjacent to the tensiometer. Combining these two shear strength formulations into one, a unique equation for the factor of safety is expressed by:

$$F_s = \frac{c'L + S \tan \phi^{\mathrm{b}} + [W \cos \psi - U + P \cos \theta] \tan \phi'}{W \sin \psi - P \sin \theta} \tag{7}$$

where W = weight of failing material, U = hydrostatic uplift force on the saturated portion of the failure surface, S = suction force on the unsaturated portion of the failure surface, P = resultant of the hydrostatic confining force due to the external water level, ψ = failure plane inclination and θ = angle formed by the resultant of the hydrostatic confining force with the failure surface. Hydrostatic water forces in the tension crack have been neglected as the upper bank remained under suction throughout the study period. Variations of unit weight with the water content of the material are taken into account using the function linking γ to the

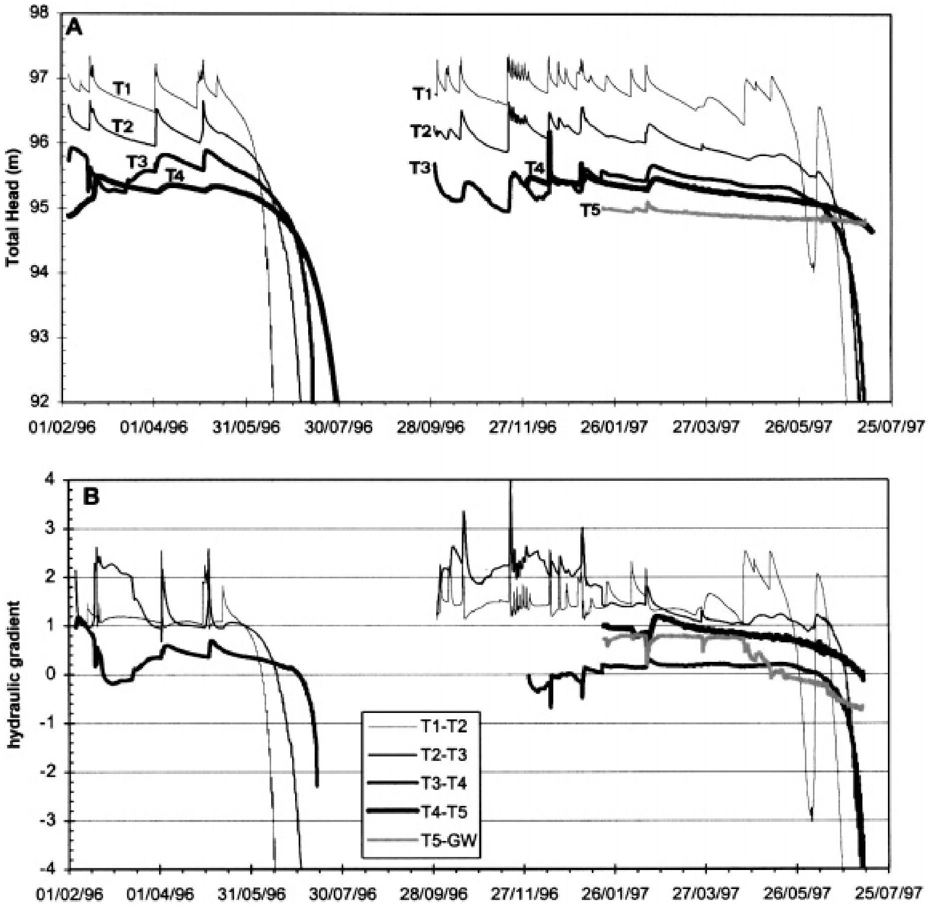

Figure 7. Changes of total head and hydraulic gradient during the 16 months of monitoring. (A) Trend of the total head. (B) Trend of the vertical hydraulic gradients

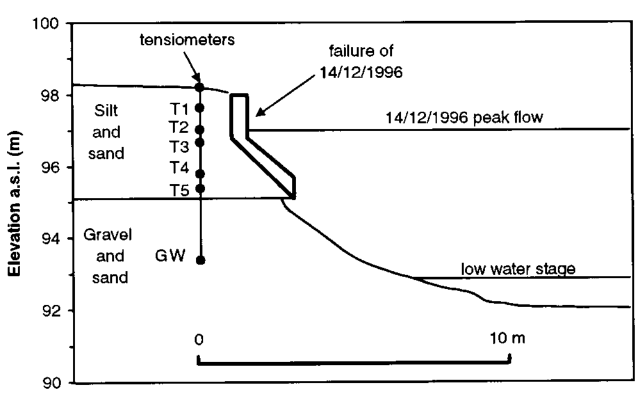

Figure 8. Geometry of the bank and mechanism of failure. T1–T5, Piezo-tensiometers; GW, piezometer

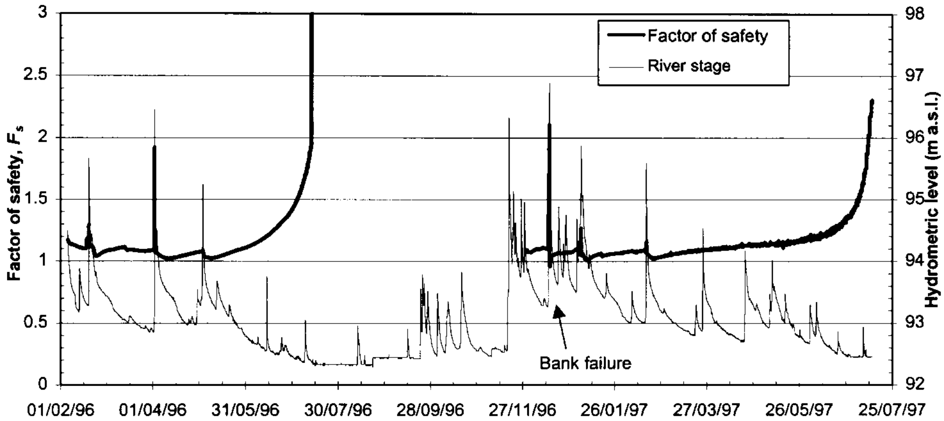

Figure 9. Trend of the safety factor (F_s) through time compared with the river stage *(H)* during the monitored period

matric suction to compute an average 'instantaneous' unit weight from the weighted average of suction values measured at the five tensiometers.

Results

The safety factor (F_s) was computed for each half hourly tensiometer reading during the monitoring period and the results are plotted with river stage in Figure 9. The seasonal variation in the curve indicates how the factor of safety responded to fluctuating matric suction. Values of F_s between February 1996 and mid-May 1996 ranged between 1 and 1·2, and fluctuated mildly in response to rainfall events. During the summer of 1996, F_s increased exponentially due to very high matric suctions. During October and November 1996, cavitation continued at T4 and this prevented calculation of the factor of safety until 27 November 1996. Between then and the end of May 1997, the factor of safety varied in the range between 1 and 1·2, as it did during the previous winter/spring period. F_s increased again in June and July 1997 as matric suction rose.

Sharp peaks in F_s values reveal that the seven major flow events that exceeded the elevation of 95·1 m a.s.l. had crucial effects on bank stability. During the rising stage of each flow event, F_s increased abruptly and during the drawdown it fell, reaching lower values than those exhibited prior to the event. The model proved capable of reproducing the observed behaviour of the bank in that it reveals that F_s fell below unity only once during the period of observation, during drawdown following the flow event of 14 December 1996, and a failure did, in fact, occur at that time.

Variation in the safety factor during the 14 December 1996 event is shown in detail in Figure 10A. A general decrease in suction at all the tensiometers (Figure 5B) produced a decrease in suction force on the unsaturated portion of the failure surface. Positive pore water pressure at T4 produced an increase in the uplift force on the saturated portion of the failure surface. Both factors decreased the stabilizing forces of the failing block. Conversely, a rise in river stage induced a significant increase in the confining pressure of water in the river. As a result of these two opposite tendencies, the factor of safety rose until the peak stage. During drawdown, suctions began to rise at all the tensiometers, although they did not recover to pre-event levels. These increases in suction were, however, insufficient to counterbalance the destabilizing effect of reduced confining pressure in the river, and the factor of safety began to decrease. During drawdown, recovery of suction took place at a slower rate than stage reduction, so that the factor of safety fell below unity and a bank failure was triggered.

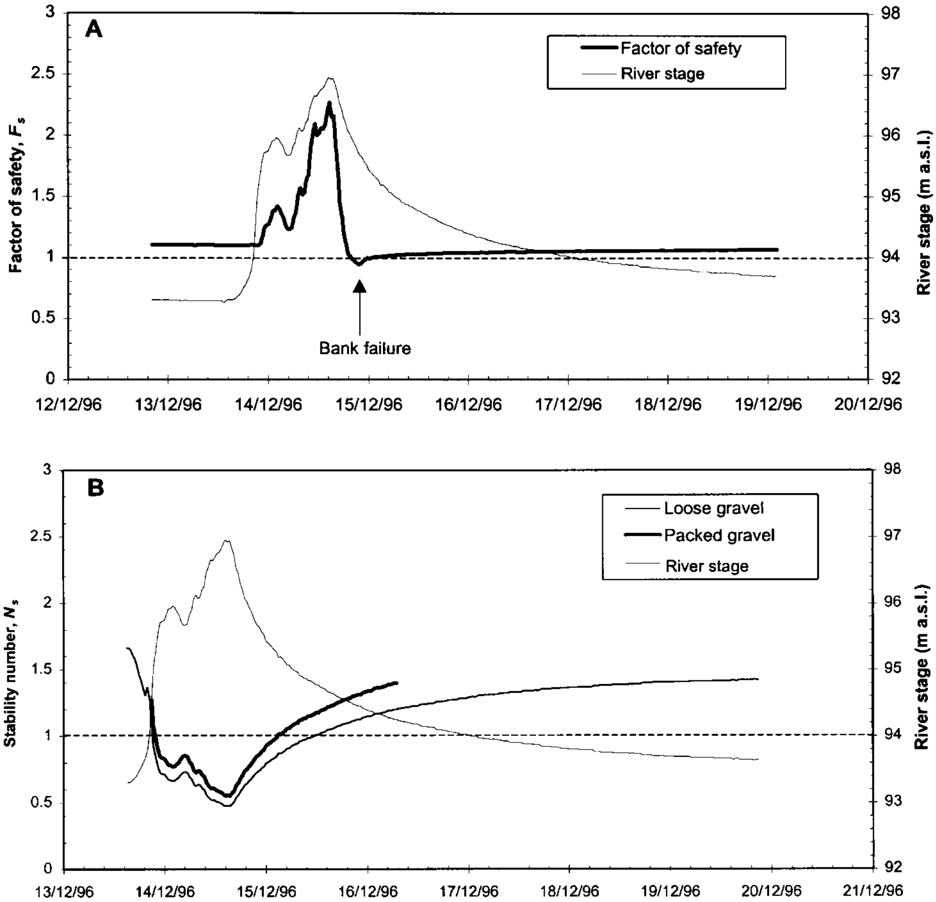

Figure 10. Bank stability and erosion during the 14 December 1996 flow event. (A) Variation in the factor of safety (F_s) compared with the river stage *(H)*. (B) Variation in the packed and loose gravel stability numbers (N_s) compared with the river stage *(H)*

FLUVIAL EROSION

Fluvial entrainment analysis

Between August 1996 and July 1997 the erosion pins were measured six times (Curini, 1998). Most pins recorded erosion on only the four measurement dates preceded by significant flow events (18 November 1996, 14 December 1996, 4 January 1997, 15 February 1997). Marked pebbles at the bank toe were completely removed by the event of 18 November 1996 and a set of replacement marked pebbles was similarly removed by the event on 14 December 1996, with the exception of a few pebbles in the size classes $-5{\cdot}5\phi/-6\phi$ and $-6\phi/-6{\cdot}5\phi$. The painted portion of the basal packed gravel was partially eroded by the flow event of 18 November 1996, and completely removed by the event on 14 December 1996.

Mean boundary shear stress at a cross-section can be calculated as:

$$\tau_o = \gamma_w RS \tag{8}$$

where τ_o = estimated boundary shear stress (N m^{-2}), γ_w = unit weight of the water (N m^{-3}), R = hydraulic radius (m) and S = energy slope (m m^{-1}).

Table III. Peak stage *(H)*, estimated mean boundary shear stress (τ_o) and shear stress on the bank (τ_b) for the four flow peaks during the period of fluvial entrainment measurements

Flow event	H(m)	τ_o (N m^{-2})	τ_b (N m^{-2})
18/11/96	3·28	67·5	50·6
14/12/96	3·66	78·2	58·6
4/01/97	2·78	55·0	41·2
15/02/97	2·57	50·6	37·9

In a wide, open channel, boundary shear stress on the basal area of the bank is approximated by (Chow, 1959, p.169):

$$\tau_b = 0 \cdot 75\ \tau_o \tag{9}$$

where τ_b = shear stress on the bank (N m^{-2}), and τ_o = mean boundary shear stress in the cross-section (N m^{-2}).

These equations were used to estimate mean boundary and bank shear stresses during the flow events that generated bank toe erosion. A reach-averaged value of 0·003 was used for the energy slope on the basis of high-flow water level observations. The results are listed in Table III.

Separate critical shear stresses were estimated for the loose and packed gravels making up the basal portion of the bank. The Lane (1955) equation, which accounts for the effects of particles resting on an inclined bank, was used to estimate critical shear stress for the loose gravel:

$$\tau_{cb} = \cos\beta\sqrt{1-(\tan\beta/\tan\phi)^2}\ \tau_c \tag{10}$$

where τ_{cb} = critical shear stress on the side slope (N m^{-2}), β = side slope angle, ϕ = friction angle and τ_c = critical shear stress on the bed (N m^{-2}). To estimate the critical shear stress, τ_c, for heterogeneous coarse sediments, the formula proposed by Komar (1987) was applied:

$$\tau_c = 0 \cdot 045(\gamma - \gamma_w){D_{50}}^{0\cdot 6}{D_i}^{0\cdot 4} \tag{11}$$

where τ_c = critical shear stress (N m^{-2}), γ = unit weight of sediment (N m^{-3}), γ_w = unit weight of water (N m^{-3}), D_{50} = median size of the sediment (m); and D_i = size representative of the coarser fraction, assumed equal to D_{84} (m).

Equation 9 is only applicable for loose material, with a side slope (β) less than the friction angle (ϕ). However, packed and cemented gravel usually display side-slope angles higher than the friction angle of sediments of the same size. To take this into account, Millar and Quick (1993) proposed the use of a modified friction angle (ϕ^*) estimated in the field from the steepest angle measured in that material. They recommend a modified formula for the critical shear stress:

$$\tau_{cb} = 0 \cdot 067\tan\phi^*\sqrt{1-(\sin\beta/\sin\phi^*)^2}\ (\gamma-\gamma_w)D_{50} \tag{12}$$

where τ_{cb} = critical shear stress on the side slope (N m^{-2}), β = side slope angle, ϕ^* = friction angle for the

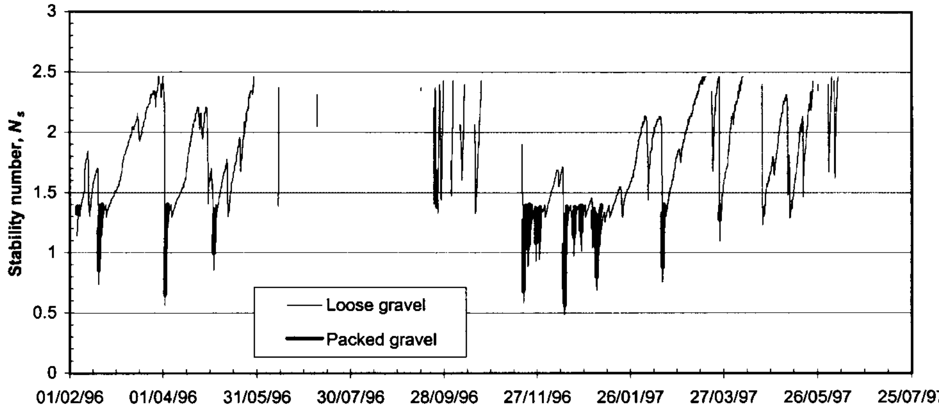

Figure 11. Variations in the loose and packed gravel stability numbers (N_s) during the monitoring period

packed sediments, γ = unit weight of the sediments (N m^{-3}), γ_w = unit weight of the water (N m^{-3}) and D_{50} = median size of the sediment (m). At the monitored bank, critical shear stress on the side slope for the loose basal gravel ($\beta = 25°$, $\phi = 35°$, $D_{50} = 0{\cdot}035$ m, $D_{84} = 0{\cdot}117$ m) and the packed gravel ($\beta = 71°$, $\phi^* = 80°$, $D_{50} = 0{\cdot}019$ m) were calculated as 27·9 N m^{-2} and 32·5 N m^{-2}, respectively. Although limitations arise in estimating critical shear stresses for bank materials (Thorne, 1982), these equations appear to provide a reasonably good prediction, since on the occasions when the erosion pins, marked pebbles and painted bank sections revealed erosion, calculated shear stresses were greater than the estimated critical values.

To illustrate temporal variation in the stability of the basal portion of the bank with respect to fluvial entrainment, a dimensionless hydraulic stability number (N_s) was derived using an approach similar to that of Watson *et al.* (1988)

$$N_s = \tau_{cb}/\tau_b \tag{13}$$

where τ_{cb} = critical shear stress on the side slope (N m^{-2}) and τ_b = shear stress on the bank (N m^{-2}). A stability number less than 1 indicates that critical conditions for fluvial entrainment are exceeded. During the monitoring period, the shear stress (τ_b) on the bank was determined using Equations 8 and 9, and separate stability numbers were computed for loose and packed gravel using critical shear stresses from Equation 10 and 12, respectively.

Results and discussion

Hydraulic stability numbers are plotted as a function of time during a single flow event in Figure 10B. The results illustrate that variations in the stability numbers (N_s) were unsynchronized with variation in the safety factor (F_s) (Figure 10A). During the rising stage, bank shear stress at the toe increased (decrease of N_s) while an increase in hydrostatic confining pressure on the bank led to an increase in the factor of safety, F_s. The most critical conditions for fluvial entrainment of gravel from the bank toe occurred at peak stage, when the fluid shear stress was greatest (minimum N_s). Conversely, the safety factor with respect to mass movement was at a maximum. The bank shear stresses decreased during drawdown (increase of N_s), while the safety factor reached a minimum. Figure 11 shows the hydraulic stability numbers for periods when the toe was inundated. The results show that stability numbers for loose and packed gravel dropped below unity on 11 and six occasions, respectively. Considering only the period during which erosion pin and marked pebble measurements were conducted (August 1996 to July 1997), stability numbers for loose and packed gravel were less than unity on eight and four occasions, respectively. These results are consistent with the

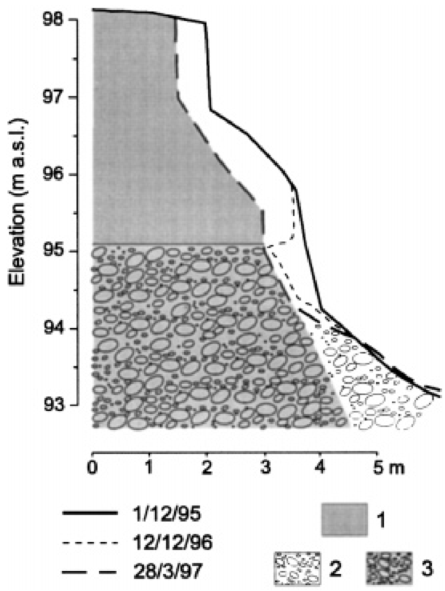

Figure 12. Repeated bank profiles 1995–1997. Key: 1, silt and sand; 2, loose gravel; 3, packed gravel with interstitial sand

observations that four erosion events were detected in the monitoring programme using the erosion pins and marked pebbles.

The monitoring data also show that the frequency of occurrence of the various erosion processes and mechanisms of failure are significantly different. During the period of monitoring, one mass failure occurred, while critical conditions for fluvial entrainment at the bank toe represent a relatively frequent event, being reached many times a year. Comparison of the bank profiles surveyed during the observation period (Figure 12) demonstrates that retreat of the bank toe due to fluvial erosion during the study period is comparable to that of the upper portion of the bank due to mass failure, although the frequencies of retreat events are significantly different. Previous studies of composite streambanks have highlighted the importance of fluvial processes in undermining the bank to generate cantilevers that subsequently collapsed by beam failure (Thorne and Lewin, 1979; Thorne and Tovey, 1981). They have also suggested that the long-term retreat rate of composite banks depends on the degree of fluvial scour at the toe through the concept of basal endpoint control. The observations made in this study differ from the earlier work in that fluvial erosion did not produce cantilevers in the upper bank during the monitoring period, but only a slight undercutting that had no measurable influence on the safety factor of the bank. However, the sequence of events responsible for bank retreat at the study site was consistent with the concept of basal endpoint control in that it consisted of:

(1) fluvial erosion to produce a steep or slightly undercut profile for the basal bank;
(2) mass failure of the upper cohesive portion of the bank triggered by reduced pore water suction and drawdown in the river;
(3) immediate removal of the failed material by the flow during the recessional part of the flood.

CONCLUSIONS

Matric suction in the unsaturated portions of a streambank has been shown to contribute significantly to the shear strength to the bank material, allowing steep or near-vertical banks to remain stable during low-flow periods. Monitoring of pore water pressures in a streambank has demonstrated that matric suction is subject to fluctuations at both the seasonal and single-event temporal scales. Rainfall infiltration, evapotranspiration,

lateral seepage due to changing river stage, and oscillations in the water table and capillary fringe are the main factors that induce changes in suction and, consequently, influence water movement in the unsaturated zone and the shear strength of the bank material. The experimental approach presented in this paper could be employed to monitor any riverbank composed of fine granular material in a humid or semi-arid climate where suction values are, for most of the year, lower than the 850 hPa instrumental upper threshold of the tensiometers. The response of pore water pressures to external factors will, however, differ depending on the soil properties, water table height, basin hydrology and hydraulic characteristics of the river.

During the monitored period, positive pore water pressures were recorded only once, during the highest flow event, and even then positive pressures only existed for a short time at the deepest tensiometer. This suggests that significant positive pore water pressures are seldom generated, even by high in-bank flows. However, reductions in matric suction were observed on many occasions and could represent an effective trigger for bank instability if they coincide with an increase in unit weight, and removal of confining pressure due to rapid drawdown in the river.

Monitoring of matric suction over a 16-month period supported application of rigorous bank stability analysis that accounted for all the factors affecting soil strength. The single planar failure that occurred in the study period was accurately explained using a new bank stability analysis that combines the Fredlund *et al.* (1978) criterion for the unsaturated portion of the bank with the normal Mohr–Coulomb criterion for the saturated portion of the failure surface, where positive pore water pressures were experienced. This finding may have a general validity for streambanks formed partly or entirely in partially saturated, fine-grained soils with properties comparable to those at the study site.

Monitoring of bank retreat confirmed that, in a composite bank, fluvial erosion events are much more frequent than bank failures. In fact, only one mass failure occurred during 16 months of monitoring, while events during which the shear stress exceeded critical shear stress for entrainment of loose and packed basal gravels occurred 11 and six times, respectively. Although the mechanics and frequencies of retreat due to erosion and failure were different, the overall retreat of the upper bank was approximately the same as that at the bank toe, as expected from the concept of basal endpoint control (Thorne and Tovey, 1981).

ACKNOWLEDGEMENTS

The research reported here was carried out at the Earth Science Department of the University of Florence under the supervision of Paolo Canuti, and funded by the Italian National Research Council Group for Hydrogeological Disaster Prevention (CNR-GNDCI). Publication CNR-GNDCI no. 1906. Nicola Casagli and Massimo Rinaldi jointly wrote most of the paper, and were responsible for the geotechnical and the geomorphic/hydraulic aspects, respectively. Alessandro Gargini was responsible for the hydrogeological aspects and contributed to the discussion section. Andrea Curini contributed to data collection and analysis as part of his postgraduate studies. Giuliano Gabbani and Pietro Vannocci, of the Earth Science Department, are acknowledged for their contributions to the general organization of the research, and for laboratory geotechnical analyses, respectively. The National Hydrological Survey of Pisa and Florence provided hydrological data. Colin R. Thorne and Damian M. Lawler are gratefully acknowledged for their thoughtful and helpful comments when refereeing the paper. The authors would finally like to thank Stephen E. Darby and Gordon Grant for their precious advice.

REFERENCES

Brooks, R. H. and Corey, A. T. 1964. Hydraulic Properties of Porous Media, Hydrology Paper No. 3, Colorado State University, Fort. Collins, Co, 27 pp.

Casagli, N., Curini, A., Gabbani, G., Gargini, A. and Rinaldi, M. 1996. 'Effetti delle pressioni interstiziali sulla stabilità delle sponde fluviali: primi risultati delle indagini sul Fiume Sieve (Toscana)', Atti V Convegno Nazionale dei Giovani Ricercatori in Geologia Applicata, (in press).

Casagli, N., Curini, A., Gargini, A., Rinaldi, M. and Simon, A. 1997. 'Effects of pore pressure on the stability of streambanks: preliminary results from the Sieve River, Italy', in Wang, S. S. Y., Langendoen, E. J. and Shields, F. D. Jr. (Eds), Management of Landscapes Disturbed by Channel Incision, Stabilization, Rehabilitation, Restoration, Center for Computational Hydroscience and Engineering, University of Mississippi, 243–248.

Chow, V. T. 1959. Open-Channel Hydraulics, McGraw-Hill Civil Engineering Series, New York.

Curini, A. 1998. Analisi dei processi di erosione di sponda nei corsi d'acqua, unpublished thesis, University of Florence, Italy, 148 pp.

Darby, S. E. and Thorne, C. R. 1996. 'Development and testing of river-bank stability analysis', *Journal of Hydraulic Engineering*, **122**(8), 443–454.

Fredlund, D. G. and Rahardjo, H. 1993. Soil Mechanics for Unsaturated Soils, John Wiley & Sons, New York, 482 pp.

Fredlund, D. G., Morgenstern, N. R. and Widger, R. A. 1978. 'The shear strength of unsaturated soils', *Canadian Geotechnical Journal*, **15**(3), 312–321.

Hooke, J. M. 1979. 'An analysis of the processes of river bank erosion', *Journal of Hydrology*, **42**, 39–62.

Huang, Y. H. 1983. Stability Analysis of Earth Slopes, Van Nostrand Reinhold, New York, 305 pp.

Komar, P. D. 1987. 'Selective gravel entrainment and the empirical evaluation of flow competence', *Sedimentology*, **34**, 1165–1176.

Köppen, W. 1936. 'Das Geographische System der Klimate', in Köppen, W. and Geiger, R. (Eds), Handbuch der Klimatologie, Bd. 1, Teil C, Berlin.

Lane, E. W. 1955. 'Design of stable channels', *Transactions of the American Society of Civil Engineers*, **120**, 1–34.

Lawler, D. M. 1991. 'A new technique for the automatic monitoring of erosion and deposition rates', *Water Resources Research*, **27**, 2125–2128.

Lawler, D. M. 1993. 'The measurement of river bank erosion and lateral channel change: a review', *Earth Surface Processes and Landforms*, **18**, 777–821.

Lawler, D. M., Thorne C. R. and Hooke, J. M. 1997. 'Bank erosion and instability', in Thorne, C. R., Hey, R. D. and Newson, M. D. (Eds), Applied Fluvial Geomorphology for River Engineering and Management, Chichester, 137–172.

Lohnes, R. A. and Handy, R. L. 1968. 'Slope angles in friable loess', *Journal of Geology*, **76**(3), 247–258.

Lutenegger, A. J. and Hallberg, G. R. 1981. Borehole Shear Test in geotechnical investigation, American Society for Testing and Materials, Special Technical Publication 740, 566–578.

Millar, R. G. and Quick, M. C. 1993. 'Effect of bank stability on geometry of gravel rivers', *Journal of Hydraulic Engineering*, **119**, 1343–1363.

Osman, A. M. and Thorne, C. R. 1988. 'Riverbank stability analysis. Part I: Theory', *Journal of the Hydraulics Division*, ASCE, **114**(2), 125–150.

Richards, L. A. 1931. 'Capillary conduction of liquid through porous medium', *Journal of Physics*, **1**, 318–333.

Rinaldi, M. 1995. Dinamica di un alveo fluviale antropizzato: il Fiume Sieve (Toscana), unpublished PhD Thesis, University of Perugia, Italy, 223 pp.

Rinaldi, M. and Casagli, N. 1999. 'Stability of streambanks formed in partially saturated soils and effects of negative pore water pressures: the Sieve River (Italy)', *Geomorphology*, **26**, 253–277.

Rinaldi, M. and Rodolfi, G. 1995. 'Evoluzione Olocenica della pianura alluvionale e dell'alveo del Fiume Sieve nel Mugello (Toscana)', *Geografia Fisica e Dinamica Quaternaria*, **18**, 57–75.

Selby, M. J. 1982. Hillslope Materials and Processes, Oxford University Press, Oxford.

Sharp, J. M. 1977. 'Limitations of bank storage model assumptions', *Journal of Hydrology*, **35**, 31–47.

Simon, A. and Darby, S. E. 1997. 'Bank erosion processes in two incised meander bends: Goodwin Creek, Mississippi', in Wang, S. S. Y., Langendoen, E. J. and Shields, F. D. Jr (Eds), Management of Landscapes Disturbed by Channel Incision, Stabilization, Rehabilitation, Restoration, Center for Computational Hydroscience and Engineering, University of Mississippi, 256–261.

Simon, A., Wolfe, W. J. and Molinas, A. 1991. 'Mass-wasting algorithms in an alluvial channel model', Proceedings of the 5th Federal Interagency Sedimentation Conference, Las Vegas, Nevada, 2, 8–22–8–29.

Springer, F. M. Jr., Ullrich C. R. and Hagerty D. J. 1985. 'Streambank stability', *Journal of Geotechnical Engineering*, **111**(5), 624–640.

Terzaghi, K. 1923. 'Die Berechnung der Durchlassigkeistziffer des Tones aus Dem Verlauf der Hydrodynamichen Spannungserscheinungen Akedemie der Wissenschaften in Wien', *Matematisch-Naturwissen-Shaftliche Klasse. Sitzungsberichte. Abteilung II*, V, **132**(3/4), 125–138.

Thorne, C. R. 1982. 'Processes and mechanisms of River Bank Erosion', in Hey, R. D., Bathurst, J. C. and Thorne, C. R. (Eds), Gravel-Bed Rivers: Fluvial Processes, Engineering and Management, J Wiley and Sons, Chichester, 227–271.

Thorne, C. R. and Lewin, J. 1979. 'Bank processes, bed material movement and planform development in a meandering river', in Rhodes, D. D. and Williams, G. P. (Eds), Adjustments of the Fluvial System, Kendall/Hunt Publishing, Dubuque, Iowa, 117–137.

Thorne, C. R. and Tovey, N. K. 1981. 'Stability of composite river banks', *Earth Surface Processes and Landforms*, **6**, 469–484.

Twidale, C. R. 1964. 'Erosion of an alluvial bank at Birdwood, South Australia', *Zeitschrift für Geomorphologie*, **8**, 189–211.

Wagner, A. A. 1957. 'The use of the Unified Soil Classification System by the Bureau of Reclamation', Proceedings 4th International Conference on Soil Mechanics and Foundation Engineering (London), 1, 125.

Watson, C. C., Harvey, M. D., Biedenharn, D. S. and Combs, P. G. 1988. 'Geotechnical and hydraulic stability numbers for channel rehabilitation: Part I & II', in Gessler, J. and Abt, S. R. (Eds), Hydraulic Engineering, ASCE, 120–131.

